

# Mechanistic cross-talk between DNA/RNA polymerase enzyme kinetics and nucleotide substrate availability in cells: Implications for polymerase inhibitor discovery

Received for publication, June 5, 2020, and in revised form, July 31, 2020. Published, Papers in Press, July 31, 2020, DOI 10.1074/jbc.REV120.013746

Si'Ana A. Coggins<sup>1,‡</sup>, Bijan Mahboubi<sup>1,‡</sup> , Raymond F. Schinazi<sup>1</sup>, and Baek Kim<sup>1,2,\*</sup> 

From the <sup>1</sup>Department of Pediatrics, School of Medicine, Emory University, Atlanta, Georgia, USA and the <sup>2</sup>Center for Drug Discovery, Children's Healthcare of Atlanta, Atlanta, Georgia, USA

Edited by Craig E. Cameron

Enzyme kinetic analysis reveals a dynamic relationship between enzymes and their substrates. Overall enzyme activity can be controlled by both protein expression and various cellular regulatory systems. Interestingly, the availability and concentrations of intracellular substrates can constantly change, depending on conditions and cell types. Here, we review previously reported enzyme kinetic parameters of cellular and viral DNA and RNA polymerases with respect to cellular levels of their nucleotide substrates. This broad perspective exposes a remarkable co-evolution scenario of DNA polymerase enzyme kinetics with dNTP levels that can vastly change, depending on cell proliferation profiles. Similarly, RNA polymerases display much higher  $K_m$  values than DNA polymerases, possibly due to millimolar range rNTP concentrations found in cells (compared with micromolar range dNTP levels). Polymerases are commonly targeted by nucleotide analog inhibitors for the treatments of various human diseases, such as cancers and viral pathogens. Because these inhibitors compete against natural cellular nucleotides, the efficacy of each inhibitor can be affected by varying cellular nucleotide levels in their target cells. Overall, both kinetic discrepancy between DNA and RNA polymerases and cellular concentration discrepancy between dNTPs and rNTPs present pharmacological and mechanistic considerations for therapeutic discovery.

Both RNA and DNA polymerases have been well-studied with respect to their structural and mechanistic properties. Generally, polymerization consists of an initial DNA or RNA template-binding step, an elongation step in which the polymerase binds and incorporates incoming dNTP or rNTP substrates, and a termination step. RNA polymerases, which can be classified through their primer-dependent or primer-independent (*de novo*) initiations, differ from DNA polymerases, which are all primer-dependent (1–3). The variety of initiation mechanisms for viral RNA polymerases include cap-snatching, template-primed, protein-primed, *de novo*, or a combination of these (4, 5).

Structural analysis and enzyme kinetic assays have provided insight into the differential mechanisms involved in the substrate specificity and binding efficiency of various viral and cel-

lular polymerases (6–9). Kinetic parameters can be used to compare the enzymatic activities of different polymerases and are determined in steady state (observes product formation in the presence of equimolar enzyme and enzyme-substrate complexes) or pre-steady state (observes the formation and consumption of enzyme-substrate intermediates) conditions, respectively (10). Here, we discuss the significance of DNA and RNA polymerase enzyme kinetics in the scope of the availability of nucleotide substrates, which can vary significantly in cells. Also, because nucleoside/nucleotide analogs, which are extensively used as anti-cancer and anti-viral pathogen agents, compete against cellular natural nucleotides, we discuss the interplay between cellular nucleotide availability and the efficacy of these analogs.

## Variations in cellular dNTP availability

During the cell cycle, cellular dNTP pools are carefully regulated by enzymes that either degrade or synthesize dNTP molecules in preparation for various cell cycle checkpoints. In S phase, expression of dNTP biosynthesis machinery, such as ribonucleotide reductase and thymidine kinase, is up-regulated, enabling the completion of DNA replication and dNTP consumption prior to mitotic division (11–14). Whereas sterile  $\alpha$  motif (SAM) domain and histidine-aspartate domain (HD)-containing protein 1 (SAMHD1) is constitutively expressed throughout the cell cycle (15, 16), dNTP degradation by the enzyme peaks during G<sub>1</sub> to aid in G<sub>1</sub>/S transition (17). Although essential for other cellular processes (18, 19), dNTPs are commonly thought of as the building blocks of DNA. dNTP molecules are incorporated into nascent DNA, primarily during DNA replication in S phase; thus, physiological concentrations of cellular dNTPs dictate the replicative capacity of any given cell. As such, nucleotide concentrations in tumor cells (7.2–32  $\mu\text{M}$ ) and transformed cell lines (3.3–79  $\mu\text{M}$ ) with uncontrolled cell cycles are nearly 5-fold greater than those found in normal resting cells (1.5–5.4  $\mu\text{M}$ ) yet similar to those found in actively dividing cells (5.2–37  $\mu\text{M}$ ) (Table 1) (20, 44). Indeed, constitutively elevated cellular dNTP pools are considered a biomarker of transformed tumorigenic cells and result from a large proportion of the cell population undergoing S phase DNA replication and peak dNTP synthesis (45–47).

Terminally differentiated/nondividing cells like macrophages do not undergo mitotic division and thus have no necessity to

<sup>‡</sup>These authors contributed equally to this work.

\* For correspondence: Baek Kim, baek.kim@emory.edu.

This is an Open Access article under the [CC BY](https://creativecommons.org/licenses/by/4.0/) license.

**Table 1****Average human intracellular dNTP concentrations and  $K_m$  values of cellular and viral DNA polymerases**

	dATP	dTTP	dCTP	dGTP	References
Average intracellular concentrations ( $\mu\text{M}$ )					
<b>Cell type</b>					
Dividing cell <sup>a</sup>	24 $\pm$ 22	37 $\pm$ 30	29 $\pm$ 19	5.2 $\pm$ 4.5	20
Resting cell <sup>a</sup>	3.2 $\pm$ 3.4	5.4 $\pm$ 6.4	2.1 $\pm$ 2.7	1.5 $\pm$ 1.0	20
Tumor cell <sup>a</sup>	23 $\pm$ 22	32 $\pm$ 24	29 $\pm$ 20	7.2 $\pm$ 4.4	20
Resting T cells <sup>b</sup>	0.32 $\pm$ 0.02	0.31 $\pm$ 0.02	0.35 $\pm$ 0.01	0.28 $\pm$ 0.02	21
Activated T cells <sup>b</sup>	1.63 $\pm$ 0.21	2.53 $\pm$ 0.16	1.89 $\pm$ 0.13	1.45 $\pm$ 0.20	21
Macrophages <sup>b</sup>	0.062 $\pm$ 0.008	0.084 $\pm$ 0.014	0.081 $\pm$ 0.008	0.051 $\pm$ 0.009	21
All human cells <sup>c</sup>	2.4	17.0	4.5	2.7	20
$K_m$ ( $\mu\text{M}$ ) <sup>d</sup>					
<b>Polymerase</b>					
Human pol $\alpha$	0.20–3.00	1.4–4.00	0.90–2.30	0.16–2.20	22–27
Human pol $\delta$ <sup>e</sup>	2.10	6.60	1.20–1.40	2.50	28, 29
Human pol $\epsilon$	4.70–9.60 (dNTPs) <sup>f</sup>	2.50	— <sup>g</sup>	—	30, 31
HSV-1	0.23–0.42	0.66–7.60	0.42–2.60	0.15–2.30	22, 32–35
EBV	10.50	13.00	9.10	6.20	32, 36
HBV RT	0.12	0.04–0.31	0.09–0.22	0.05–0.40	37–40
HIV-1 RT	0.06–0.10	0.04–0.06	0.01–0.30	0.02–0.07	21, 38, 41–43

<sup>a</sup> Quantified from various mammalian cell sources.<sup>b</sup> Quantified from primary human cells.<sup>c</sup> Average of various primary and transformed human cells, excluding blood-forming cells.<sup>d</sup> Ranges consist of the mean  $K_m$  values reported in the cited publications.<sup>e</sup> Human pol  $\delta$  without PNCA.<sup>f</sup> Experiments were performed in the presence of all four dNTPs.<sup>g</sup> —, not reported.

support chromosomal DNA synthesis. Indeed, human primary monocyte-derived macrophages display 125–250-fold lower (20–40 nM) dNTP concentrations than activated human CD4<sup>+</sup> T cells (2–5  $\mu\text{M}$ ) (Table 1) (21). The extremely low dNTP pools found in nondividing macrophages result from both a lack of dNTP biosynthesis and abundant expression of active dNTPase SAMHD1 (48, 49). In addition, it is important to note that cellular dNTP pools are not comprised of equimolar concentrations of the five different nucleotides. Rather, when excluding blood-forming cells, human cells contain on average 2.4, 17, 4.5, 2.7, and 0.7  $\mu\text{M}$  concentrations of dATP, dTTP, dCTP, dGTP, and dUTP, respectively (Table 1). Availability of the correct dNTP substrate is crucial during the DNA replication process to avoid misincorporations and mismatch extension events that result in genomic mutagenesis if not properly repaired (50).

Extensive studies have been conducted to accurately determine the cellular dNTP concentrations of various cell types. As a result, there are currently multiple methods used to measure and report intracellular dNTP concentrations with the most common being liquid chromatography tandem MS (LC–MS/MS) methods and DNA polymerase-based enzymatic assays (51). With the numerous dNTP quantification tools, each comes with a unique challenge. For example, whereas LC–MS/MS accurately determines dNTP levels, this assay requires separation of mono-, di-, and triphosphate molecules via LC prior to quantification by MS/MS, making this a labor-intensive and expensive method of dNTP measurement (52, 53). Conversely, pitfalls in enzyme-based quantification methods result from the fact that DNA polymerases vary in their substrate specificity and sensitivity, often incorporating the wrong dNTP substrate or lacking polymerization activity in low-dNTP environments (54). Current polymerase-based dNTP measurement tools overcome this issue by utilizing HIV-1 reverse transcriptase in quantification assays, exploiting the viral polymerase for its unique ability to polymerize in low dNTP concentrations

unlike the Klenow polymerase, which was previously used in similar assays (21). HIV-1 reverse transcriptase will be discussed in further detail later in this review, which compiles dNTP measurement collected using a variety of the aforementioned quantification methods. Interestingly, the mitochondrial membrane serves as an effective barrier that creates differential dNTP concentrations in mitochondrial and cytoplasmic cellular compartments, resulting in two distinct dNTP pools that can be independently quantified (44). This review will not discuss mitochondrial dNTP pools or DNA polymerase  $\gamma$  kinetics; rather, it will explore viral and nuclear DNA polymerase kinetics with regard to intracellular (nuclear and cytoplasmic) dNTP availability. Whereas concentrations for metabolites in fluids are often reported in molarity (e.g.  $\mu\text{M}$ ), physiological dNTP concentrations are often reported in pmol/10<sup>6</sup> cells for cultured cells or nmol/g wet weight for tissues and require a measurement of intracellular volume for conversion to molarity (20). Further documentation of this cell-dependent variable in a variety of cultured and primary cells would be invaluable in the determination of applicable dNTP concentration data, providing a clearer understanding of intracellular conditions for pharmacological applications and kinetics studies that seek to define the substrate or ligand affinity of an enzyme in relation to the physiological concentrations of those molecules. More specifically, thorough and accurate documentation of intracellular dNTP concentrations could provide context for the enzyme kinetic parameters that have been reported for numerous cellular and viral DNA polymerases that function in a variety of diverse cellular and tissue environments.

### DNA polymerase kinetics: Cellular and viral DNA polymerases

DNA polymerases synthesize DNA through replication of genomic materials in the form of DNA or RNA templates (55,

56). This process consumes cellular dNTPs; thus, the rate of DNA synthesis is kinetically dependent upon intracellular dNTP availability that can vary, depending on cell type. Therefore, it is a reasonable assumption that DNA polymerases have been kinetically optimized through evolution to properly support cellular DNA synthesis. In other words, exposure to cell-specific substrate conditions can drive DNA polymerase evolution and kinetics. Steady-state kinetic parameter  $K_m$  represents the substrate concentration needed for the enzyme to operate at half the  $V_{max}$  and is commonly used to compare the operation capabilities of enzymes that catalyze the same chemical reactions at given substrate concentrations. Here, we reviewed the published  $K_m$  values of many cellular and viral polymerases.

Human replicative DNA polymerases (pols)  $\alpha$ ,  $\delta$ , and  $\epsilon$  are responsible for accurately and efficiently replicating the majority of genomic DNA in dividing cells (57). Whereas the  $K_m$  values of dNTP incorporation by pol  $\alpha$  have been reported to be in the range of 0.16–4.00  $\mu\text{M}$  (Table 1), pol  $\epsilon$  synthesizes DNA with a  $K_m$  of 2.5–9.6  $\mu\text{M}$  (30, 31). Similarly, replicative DNA polymerase  $\delta$  displays  $K_m$  values ranging from 1.2 to 6.6  $\mu\text{M}$  (28); however, this is reduced to 0.067  $\mu\text{M}$  in the presence of proliferating cell nuclear antigen, an essential processivity factor that recruits pol  $\delta$  to the replication site and increases polymerase binding to the DNA template (29, 58, 59). Interestingly, the larger  $K_m$  values associated with incorporation of dTTP by these replicative polymerases agree with the large relative concentrations of dTTP within the intracellular dNTP pools of a normal dividing cell (Table 1). However, replicative DNA polymerases are not the only polymerases with  $K_m$  values coinciding with dNTP availability within dividing cells. DNA polymerase  $\beta$  is known to be involved in base excision repair, or gap-filling DNA synthesis, and has been reported to have a  $K_m$  value as low as 1.7  $\mu\text{M}$  and as high as 31  $\mu\text{M}$ , depending on the template sequence and dNTP substrate (22–24, 32, 36, 60). In 2001, Vande Berg *et al.* (61) found that the  $K_m$  associated with gap-filling DNA synthesis using a gapped template ( $0.18 \pm 0.02 \mu\text{M}$ ) was 12-fold lower than when utilizing a nongapped substrate ( $2.36 \pm 0.75 \mu\text{M}$ ). DNA pols  $\delta$  and  $\beta$  display relatively lower  $K_m$  values through two differential means that are independent of intracellular dNTP concentration—interaction with an accessory protein or preferential binding to a template substrate, respectively. Overall,  $K_m$  values of cellular replicative DNA polymerase are close to dNTP concentrations found in dividing cells, supporting a possibility of the kinetic adaptation of these host replicative DNA polymerases to optimally support host chromosomal DNA replication at the dNTP concentrations found in dividing cells.

Many viruses replicate their viral DNA genomes within target host cells by using the dNTPs available within the infected cells. Herpes simplex virus 1 (HSV-1) is able to infect a variety of cell types ranging from epithelial cells to neurons. HSV-1 polymerase incorporates individual dNTPs with  $K_m$  values ranging from 0.15 to 7.6  $\mu\text{M}$  (Table 1) or  $1.1 \pm 0.07 \mu\text{M}$  for all dNTPs (62). Importantly, rather than replicating in normal dNTP conditions, HSV-1 encodes a viral ribonucleotide reductase protein that increases intracellular dNTP concentrations during viral replication. It is possible that the possession of its own dNTP biosynthesis capability enables this virus to replicate even in

nondividing cells with poor dNTP availability, such as neurons. Like HSV-1, Epstein–Barr Virus (EBV) encodes its own dNTP biosynthesis machinery that provides dNTPs for its viral DNA genome replication regardless of cellular dNTP biosynthesis and proliferation conditions. Increased dNTP substrate availability in EBV infections coincides with a large  $K_m$  value (6.2–13  $\mu\text{M}$ ) (Table 1). With no virus-driven dNTP biosynthesis abilities, vaccinia virus from the *Poxviridae* family and human cytomegalovirus from the *Herpesviridae* family display similar  $K_m$  values ranging from 0.90 to 3.80 (63, 64) and from 0.67 to 3.77  $\mu\text{M}$  (25, 65–68), respectively, depending on the identity of the incorporated dNTP molecule.

Hepatitis B virus (HBV) utilize a virally encoded reverse transcriptase (RT) that synthesizes DNA from both DNA and RNA templates to replicate the viral genome during the replication cycle. Liver-tropic HBV primarily targets human hepatocytes during viral infection and harbors an RT that polymerizes dNTP incorporation with relatively low  $K_m$  values (0.04–0.40  $\mu\text{M}$ ) (Table 1). Variations in reported HBV RT  $K_m$  values arise from different methods of quantifying DNA polymerase activity (37–39).

Retroviruses also employ their own RTs for RNA- and DNA-dependent DNA polymerization of the viral genome. Whereas lentiviruses, including HIV-1, replicate in both dividing and nondividing cells (69–71), other nonlentiviral retroviruses, such as murine leukemia virus (MuLV) and avian myeloblastosis virus (AMV), execute productive infection exclusively in dividing cells (72–74). Indeed, whereas MuLV and AMV RTs synthesize DNA efficiently at the dNTP concentrations found in dividing cells, these RTs failed to synthesize DNA at the low-dNTP concentrations found in nondividing macrophages (21). In contrast, HIV-1 replicates within human CD4<sup>+</sup> T cells and macrophages; thus, the cell tropism of HIV-1 is comprised of two cell types with vastly different intracellular dNTP environments. Indeed, the SAMHD1-mediated low dNTP concentrations (nanomolar range) present in macrophages can kinetically block HIV-1 proviral DNA synthesis (20, 21, 48). However, it was reported that HIV-1 RT is able to synthesize DNA even within the restrictive dNTP pools of the macrophage, an environment that completely inhibits the DNA synthesis activity of MuLV and AMV RTs. Pre-steady-state kinetic analysis demonstrated that the failure of MuLV RT to synthesize DNA within low dNTP concentrations is due to its low dNTP-binding affinity (75). Conversely, the successful DNA synthesis activity of HIV-1 RT at restrictive dNTP concentrations mechanistically results from its higher dNTP-binding affinity (75), which enables HIV-1 to complete viral reverse transcription in nondividing macrophages. Overall, these RTs may have evolved to display differential DNA polymerase kinetics to optimally support viral DNA synthesis in their target cells, ultimately contributing to their differential cell tropisms (dividing *versus* nondividing cells).

Interestingly, HIV-2 and some simian immunodeficiency virus strains target host dNTPase SAMHD1 for proteasomal degradation using virally encoded Vpr or Vpx proteins. Virus-induced SAMHD1 degradation increases intracellular dNTP pools in macrophages and enables the completion of reverse transcription in this restrictive cell type. Whereas HIV-1

cannot counteract host SAMHD1, numerous studies have identified that HIV-1 RT incorporates dNTPs into nascent DNA with a  $K_m$  of 0.01–0.30  $\mu\text{M}$  in single-nucleotide incorporation experiments while possessing an overall  $K_m$  of 0.0063  $\mu\text{M}$  when all nucleotides are present (41). As an RNA- and DNA-dependent polymerase, HIV-1 RT has been found to polymerize from an RNA template with greater efficiency than when using a DNA template (76, 77). Therefore, the high binding affinity and nanomolar range  $K_m$  value of HIV-1 RT enables slow but complete reverse transcription in the SAMHD1-mediated dNTP-depleted conditions of the nondividing macrophage. Interestingly, lentiviruses that do not possess the ability to counteract SAMHD1 have been found to harbor RTs that are more catalytically efficient and able to more quickly incorporate incoming dNTP molecules than RTs originating from lentiviruses that can counteract SAMHD1 and increase intracellular dNTP pools during viral infection (78–80). These findings imply not only that HIV-1 RT was evolutionarily honed to circumvent SAMHD1 restriction in target host macrophage cells harboring low dNTP concentrations, but also that SAMHD1 may have influenced RT kinetics among lentiviruses, depending on their anti-SAMHD1 capability that modulates intracellular dNTP levels in nondividing target cell types.

### Efficacy of anti-HIV-1 nucleotide/nucleoside reverse transcriptase inhibitors (NRTIs)

NRTIs are a class of reverse transcriptase inhibitors that mimic the molecular structure of natural nucleotides and inhibit viral reverse transcription through a variety of mechanisms, namely chain termination or translocation inhibition. The nucleotide-like structure of NRTIs (in their triphosphate forms) supports binding within the RT active site and subsequent incorporation into the nascent DNA strand during reverse transcription. In 1987, thymidine analog 3'-azido-3'-deoxythymidine 5'-triphosphate (AZT-TP) was the first anti-HIV drug to be approved by the Food and Drug Administration. The 3'-azide group enables the drug to function as a chain terminator once incorporated into viral DNA by RT. Incorporated with  $K_m$  values of 0.13–0.19 and 2.9–35.2  $\mu\text{M}$  when using RNA and DNA templates, respectively, AZT-TP was found to be a comparable substrate to dTTP during polymerization from an RNA template (Table 1) (76, 77, 81). Extensive studies of the chain-terminating drug revealed that AZT-TP selectively inhibits retroviral HIV-1 and simian immunodeficiency virus RTs (82, 83) and does not appear to be a substrate of cellular DNA polymerase, such as pols  $\alpha$ ,  $\delta$ , and  $\beta$  (60, 84, 85). In biochemical inhibitor studies, the  $\text{IC}_{50}$  of a drug indicates the drug concentration needed to reduce enzyme biochemical activity by half. Studies conducted using HIV-1 RT from various HIV-1 strains reported  $\text{IC}_{50}$  values for AZT-TP in the range of 0.02–3.20  $\mu\text{M}$ , with experiments using RT from the HIV-1 BH10 strain (HIV-1 BH10 RT) yielding substantially greater values than those conducted with HIV-1 HXB2 RT (86–92).

Like AZT-TP, cytosine analog dideoxycytosine (ddCTP) also functions as an anti-HIV chain-terminating drug. Studies show that ddCTP, also known as zalcitabine, inhibits HIV-1 RT with an  $\text{IC}_{50}$  value of 0.08–1.44  $\mu\text{M}$  (88–92). Unlike AZT-TP, zalcita-

bine displays inhibitory effects on cellular DNA polymerase  $\beta$  when provided in near- $\text{IC}_{50}$  doses (24, 60). Similarly, didanosine (ddITP) is incorporated onto nascent DNA from a DNA template with a  $K_m$  of 0.097  $\mu\text{M}$  and an  $\text{IC}_{50}$  of 0.18–0.80  $\mu\text{M}$  (89–93); however, comparable  $\text{IC}_{50}$  values are found for pol  $\beta$  when polymerizing from calf thymus DNA (94). Due to their overlapping toxicity profiles, zalcitabine and didanosine were not administered in combinations with one another prior to the discontinuance of zalcitabine in 2006.

Tenofovir (TFV-DP) is an adenosine analog that acts as a chain terminator through its lack of a 3'-carbon and subsequent 3'-hydroxyl moiety required for chain elongation. In the absence of ATP, TFV-DP inhibited HIV-1 RT polymerization with an  $\text{IC}_{50}$  value of 0.45–0.88  $\mu\text{M}$  (91, 93, 95). With ATP present to facilitate ATP-mediated excision of the chain terminator (88, 96, 97), the  $\text{IC}_{50}$  of TFV-DP is increased to 1.85  $\mu\text{M}$  (95). Interestingly, this is not the case for 4'-ethynyl-2-fluoro-2'-deoxyadenosine triphosphate (EFdA-TP). Rather than acting as a chain terminator, this adenosine analog retains a 3'-hydroxyl group and, instead, acts as a translocation-defective reverse transcriptase inhibitor that inhibits the translocation of RT once incorporated into the nascent DNA. Although aptly poised for ATP-mediated excision, EFdA-TP is reincorporated into the DNA almost immediately upon excision by ATP (91). This novel drug is incorporated by HIV-1 RT with a  $K_m$  of 0.024–0.049  $\mu\text{M}$ , depending on template type—DNA versus RNA—and the subtype of HIV-1 RT used in the study (91, 98). The  $K_m$  associated with incorporation of EFdA-TP is lower than that of the natural substrate, dATP (0.06–0.10  $\mu\text{M}$ ) (Table 1). With an  $\text{IC}_{50}$  of 0.014  $\mu\text{M}$  in HIV-1 RT systems, EFdA-TP shows no activity against cellular polymerases  $\alpha$  and  $\beta$  while slightly inhibiting mitochondrial DNA polymerase  $\gamma$  with an  $\text{IC}_{50}$  of 10  $\mu\text{M}$ —a concentration over 700-fold greater than that of HIV-1 RT (91, 94).

Comparison of the selective inhibition of HIV-1 RT by AZT-TP and EFdA-TP with the toxicity of zalcitabine and didanosine against cellular DNA polymerase  $\beta$  reveals the complicated nature of anti-retroviral drug design. Subsequent to meticulous chemical design strategies, selective targeting of viral polymerases requires careful consideration of the varying  $K_m$  values associated with incorporation of the drug by cellular and viral polymerases, the competition of NRTI molecules with endogenous cellular dNTP substrates, and the potential excision or metabolic pathways that might aid or hinder drug efficacy. Indeed, the efficacy of these NRTIs is significantly improved in nondividing macrophages compared with activated  $\text{CD4}^+$  T cells due to the SAMHD1-mediated depletion of the natural dNTP substrate that all NRTI-TP compete against in this nondividing target cell type (20, 99, 100). Whereas additional factors, such as substrate binding affinity and the rate of substrate incorporation, also influence the efficacy of an NRTI, the drug must always outcompete the cell-dependent availability of natural dNTP substrates.

### Cellular rNTP concentrations and enzyme kinetics of cellular and viral RNA polymerases

Whereas cellular dNTPs are used solely for DNA synthesis, cellular rNTPs show highly versatile utilities in cells. First, rNTPs are substrates of cellular RNA polymerases for

**Table 2**  
Average human intracellular NTP concentrations and  $K_m$  values of viral RNA polymerases

	ATP	UTP	CTP	GTP	References
	Average intracellular concentrations ( $\mu\text{M}$ )				
<b>Cell type</b>					
Dividing cell <sup>a</sup>	3,152	567	278	468	20
Resting cell <sup>a</sup>	2,537	227	83	232	20
Tumor cell <sup>a</sup>	3,134	686	402	473	20
	$K_m$ ( $\mu\text{M}$ ) <sup>b</sup>				
<b>Polymerase</b>					
HCV	2.34 ± 0.07	1.51 ± 0.02	0.24 ± 0.01	1.85 ± 0.28	103
DENV	2.25 ± 0.84	— <sup>c</sup>	—	0.37 ± 0.07	104
IAV	33.22 ± 3.37	22.01 ± 1.48	28.93 ± 0.48	10.74 ± 0.26	105
EBOV	1.5 ± 0.23	—	1.2 ± 0.11	—	106
MERS	0.017 ± 0.0019	—	—	—	106
SARS	0.03 ± 0.003	—	—	—	106
SARS2	0.03 ± 0.003	—	—	—	106

<sup>a</sup> Quantified from various mammalian cell sources.

<sup>b</sup>  $K_m$  values recorded during the elongation phase.

<sup>c</sup> —, Not reported.

transcription. Second, rNTPs, especially ATP and GTP, play key regulatory roles in a wide variety of cell signaling pathways. Third, ATP is an energy unit that controls numerous biological, chemical, and dynamic processes in living cells (101, 102). Intracellular rNTP concentrations are close to millimolar ranges (Table 2), which are 100–1,000 times higher than dNTP concentrations regardless of cell cycle stage (20, 107). This cellular abundance of rNTPs accommodates diverse and high cellular demands.

Unlike DNA polymerases, cellular DNA-dependent RNA polymerases initiate RNA synthesis from their promoter sequences in a primer-independent manner during transcription. This distinct method of polymerization initiation often causes methodological difficulties in polymerase enzyme kinetic analyses due to the presence of a threshold rather than a biological curve for nucleotide incorporation. However, bacterial, cellular, and phage RNA polymerases have been extensively investigated for their enzyme kinetics. Most bacterial and phage RNA polymerases, such as *E. coli* and T7 phage RNA polymerases, respectively, display high micromolar ranges of  $K_m$  values (300–900  $\mu\text{M}$ ) analogous to reported rNTP concentrations for initiation (108–111). Interestingly, these relatively high  $K_m$  values correlate with elevated intracellular rNTP concentrations within *E. coli* (0.5–3.5 mM) (102, 112, 113).

Analysis of mammalian cellular DNA-dependent RNA polymerase enzyme kinetics is scarcely reported, potentially due to the structural complexity of eukaryotic RNA polymerases that require diverse, differential, and numerous regulatory co-factors for initiation and elongation during RNA synthesis. However, multiple RNA-dependent RNA polymerases (RdRPs) of viruses that infect human cells have been investigated for their elongation steady-state enzyme kinetics using simple primer-dependent RNA polymerase activity assays. This is because these viral RdRPs can enzymatically initiate RNA synthesis without regulatory factors (114, 115). Table 2 summarizes the  $K_m$  values of these viral RdRPs. Overall, it appears that viral RdRPs display higher  $K_m$  values, compared with cellular DNA polymerases, which may be related to the highly abundant rNTP concentrations present within the cell.

Importantly, many viral RdRPs have been extensively investigated as antiviral targets, and numerous nucleotide/nucleoside analogues have been tested for their antiviral activity that block viral RNA synthesis (116). As discussed earlier with dNTPs, the efficacy of ribonucleotide/nucleoside inhibitors can be affected by the concentrations of cellular rNTPs that these analogues compete against during viral RNA genome synthesis catalyzed by viral RdRPs. It is logical to consider that the development of effective viral RdRP ribonucleotide/nucleoside inhibitors could be more challenging compared with that of deoxynucleotide/nucleoside inhibitors against DNA polymerases simply because intracellular rNTP concentrations are much higher than dNTP concentrations. Furthermore, due to other utilities of rNTPs in cells, ribonucleotide/nucleoside analogues can generate more nonspecific cellular toxicity. To overcome the intrinsically high competition with natural rNTP substrates and preserve the highly diverse utilities of rNTPs within the cell, ribonucleotide/nucleoside analogues targeting viral RdRPs should display much higher specificity against viral RdRPs without unwanted interruption of natural rNTP cellular functions. Interestingly, some viruses have adapted stages during RNA synthesis that require unusually high concentrations of rNTPs to proceed.

### Flaviviridae RdRP kinetics

The initiation of RNA synthesis, which represents the rate-limiting step, serves as a barrier for *de novo* synthesis in flaviviruses and is heavily reliant on rNTP concentrations. GTP, the second nucleotide to be incorporated during RNA synthesis, is required to be unusually high for *de novo* synthesis to occur, a common characteristic seen across the *Flaviviridae* family. Both hepatitis C virus (HCV) and dengue virus (DENV) are the best-studied disease-causing flaviviruses. HCV NS5B protein is a well-studied RdRP that utilizes two rNTP-binding pockets inside the catalytic site, one that recognizes the initiating rNTP and the second for the complementary rNTP that corresponds to the second template nucleotide (6, 117). Untranslated positive-strand HCV RNA genomes can serve as templates for further RNA replication or be assembled into virions (118). *De novo* synthesis is the process in which NS5B initiates primer-independent RNA synthesis and is initiated by the incorporation

of a single GTP molecule—an event characterized by a  $K_m$  value of 40  $\mu\text{M}$  (119). Following transcription initiation, elongation proceeds with  $K_m$  values ranging from 0.24 to 2.34  $\mu\text{M}$ , depending on the identity of the incorporated rNTP (Table 2). The 40-fold divergence in the  $K_m$  values associated with GTP incorporation during transcription initiation and elongation represents the stark difference in concentration requirements for these two phases of RNA synthesis. It is important to note that the reported  $K_m$  values calculated *in vitro* do not indicate the concentration required for *in vivo* environments because several factors have been demonstrated to affect NS5B substrate affinity for GTP (e.g. divalent cation concentrations) (114). Initiation of RNA synthesis proved to require higher GTP concentrations (>100  $\mu\text{M}$ ) regardless of the starting template nucleotide, suggesting that GTP plays a role as a structural regulator for NS5B. Additionally, the authors noted that at high concentrations, the other rNTPs were able to initiate *de novo* synthesis only in the absence of GTP (119–121). This suggests that only in nonphysiological conditions can the other rNTPs participate as the initiation nucleotide. The elongation  $K_m$  values represent the polymerization step that is not hindered by rNTP concentrations due to the relatively abundant rNTP levels that are sufficient for preventing enzymatic delays.

DENV is a single-stranded positive-sense RNA virus. DENV NS5 is a nonstructural protein with RdRP and methyltransferase activity performed via separate protein domains that are connected by a linker. *De novo* initiation for minus strand RNA synthesis is mediated by secondary viral RNA structures that guide the NS5 complex to the 3' end of the genome (122). Once positioned at the 3' end of the viral RNA, NS5 is then able to position the initiating nucleotide (ATP) into the priming site, followed by a GTP molecule, which yields the pppAG primer (123, 124). The involvement of GTP and ATP in the formation of the initiation primer suggests that there will be two  $K_m$  values for each nucleotide: one for transcription initiation and another for transcript elongation. The  $K_m$  values associated with incorporation of GTP and ATP during elongation are 0.37 and 2.25  $\mu\text{M}$ , respectively (Table 2). Unlike HCV NS5B, DENV NS5 incorporates the initiating ATP molecule with a  $K_m$  of  $5.43 \pm 2.50 \mu\text{M}$ , a concentration only 2-fold higher than what is required during elongation (104). The  $K_m$  for GTP during *de novo* initiation has not been calculated because GTP is reportedly required to be present in concentrations much greater than 100  $\mu\text{M}$  to produce transcription product (104, 125).

In studies investigating both HCV and DENV RdRPs, low-affinity GTP-specific binding sites have been identified and characterized as possible points of stabilization for a polymerase conformation that supports efficient transcription initiation (123, 126). Analysis of the *Flaviviridae* RdRPs during RNA synthesis revealed that these enzymes undergo a closed-to-open conformational change during the transition from initiation to elongation (104, 127). In the “closed” state, the enzyme is only able to accommodate a single-stranded RNA template and the incoming nucleotide in the catalytic core (127, 128). This tight conformation found in primer-independent RdRPs restricts the flexibility of producing a second RNA strand, requiring a transition to an “open” state for transcript elongation (129, 130). Because the closed-to-open transition of the viral RdRPs

is an essential step for viral replication, targeting the GTP-specific binding pocket with inhibitors has been identified as a possible drug mechanism (131). The low affinity of the binding pocket to GTP suggests the possible utilization of competitive inhibitors against that site to prevent the conformational change between “open” and “closed” states (132). A unique feature of primer-independent RdRPs is the presence of a biphasic profile as a result of the  $K_m$  gap between the incorporation of the initiation nucleotide and elongation rNTPs. The absence of a selective pressure for these viral RdRPs lies in the relatively high concentrations of cellular rNTPs. While the substrate affinity in RdRPs during elongation is severalfold lower than what is observed in DNA polymerases, the preference for rNTPs remains thousands of times separated from dNTPs (133, 134). Preference for rNTPs is further enhanced intracellularly due to the high rNTP/dNTP ratio (105, 135, 136).

### Influenza virus RdRP kinetics

Influenza A virus (IAV) contains a single-stranded, fragmented RNA genome of negative-sense polarity. The IAV RdRP is a heterotrimeric complex that hijacks capped host RNAs as a primer for mRNA viral transcription, whereas synthesis of genomic RNA is primer-independent and relies solely on *de novo* initiation (137). The molecular switch that controls the IAV RdRP to synthesize transcripts or genomic RNA is still not clear; however, studies suggest that viral protein levels might play a key role. *De novo* transcription initiation is proposed to be heavily influenced by high rNTP concentrations and favors the production of genomic RNA (119, 138, 139). Similar to HCV, *de novo* initiation of IAV replication requires the incorporation of an initiating nucleotide, often GTP or ATP, with a concentration above 100  $\mu\text{M}$ . During conditions of lower ATP, GTP, and CTP concentrations, the reaction has been shown to favor transcription via primer extension with a  $K_m$  between 10 and 30  $\mu\text{M}$  (Table 2) (140, 141). This suggests that the abundance of the initiating nucleotide might dictate the molecular switch between genomic RNA and viral mRNA transcript synthesis.

### Efficacy of viral RdRP inhibitors

In steady-state kinetic drug studies, the ratios of  $V_{\text{max}}/K_m$  for a single nucleotide over that of the associated drug analog is defined as drug selectivity. Antiviral drugs against RNA viruses are most effective when viral RdRP selectivity for the drug is high and the host RNA polymerase selectivity for the drug is low. Remdesivir is an adenosine nucleotide analog prodrug that interferes with RdRP activity through a delayed chain termination mechanism. Remdesivir has demonstrated broad-spectrum antiviral activity and thus has been tested against a variety of RNA viruses. Recently, the Götte group (106) determined that Ebola virus (EBOV) RdRP incorporates ATP with a  $K_m$  value of 1.5  $\mu\text{M}$ . Under the same conditions, the  $K_m$  value describing incorporation of remdesivir-triphosphate (TP) was calculated to be  $\sim 6 \mu\text{M}$ , with only slight discrimination against the natural ATP substrate (142).

In a study aimed at comparing the activity of several adenosine analogues against Middle East respiratory syndrome

coronavirus (MERS-CoV), remdesivir-TP stood out not only because it was the most efficiently incorporated drug within the compound panel ( $K_m = 0.0063 \mu\text{M}$ ), but also because it was more efficiently incorporated than a natural ATP substrate ( $K_m = 0.017 \mu\text{M}$ ) (143). In contrast, ATP analogues ara-ATP and 2'C-methyl-ATP (2'CM-ATP) were found to be incorporated with far less selectivity (>150-fold) than a natural ATP substrate (143). Whereas the data demonstrating the preference for remdesivir-TP over natural ATP are promising, the rNTP concentrations used to calculate the kinetic values ( $0.02\text{--}0.25 \mu\text{M}$ ) were 10,000-fold lower than physiological conditions ( $2,102 \mu\text{M}$ ) (Table 2) (20). Additionally, although the incorporation of the delayed terminating drug remdesivir-TP is successful, there is still opportunity to overcome the arrest. The mechanism of delayed termination halts the RdRP after the third nucleotide following remdesivir-TP incorporation, and the percentage of RdRP that overcomes this arrest is partially related to rNTP concentrations. Because the rate of incorporation of remdesivir-TP drops considerably as we approach physiological concentrations, we can infer that there is marginal antiviral efficacy at physiological/cellular conditions. Additionally, the biochemical assessment of remdesivir-TP potency lacks many of the variables present during *in vivo* settings. Studies have shown inconsistency in remdesivir-TP potency related to the cell types used in experiments (144). Several features noted during analysis suggested that differing outcomes could possibly be a result of cellular drug metabolism or uptake (145).

Similarly, severe acute respiratory syndrome coronavirus (SARS-CoV) and the novel coronavirus, SARS-CoV-2, RdRPs both demonstrated sensitivity to remdesivir-TP at the same capacity as the MERS-CoV RdRP, incorporating the drug with  $K_m$  values of  $0.0012\text{--}0.0023 \mu\text{M}$  (106). In all three cases, remdesivir-TP caused delayed chain termination 3 bases downstream of the drug incorporation site. Whereas the selectivity of SARS-CoV-2 RdRPs for remdesivir-TP was favorable, at physiological rNTP concentrations, there could be a reduction of the inhibitory effect. Experiments that gradually increased the concentration of the rNTP following the remdesivir-TP incorporation site resulted in a significant reduction of terminated products. Furthermore, the maximum rNTP concentration used to determine the surmountable drug effects during this study was  $10 \mu\text{M}$ , still 100-fold less than the average physiological rNTP concentration. Even under conditions with substantially lower rNTP concentrations, there was an almost complete loss of termination (106).

### Conclusions and perspectives

Comparison of intracellular dNTP and rNTP concentrations with the enzyme kinetics of cellular and viral polymerases reveals a dynamic relationship between enzyme kinetics and physiological substrate availability. Construction and expansion of a database containing intracellular nucleotide/nucleoside conditions in a variety of human and animal cell types would be beneficial to provide context for enzyme kinetics studies and aid in the discovery and development of competi-

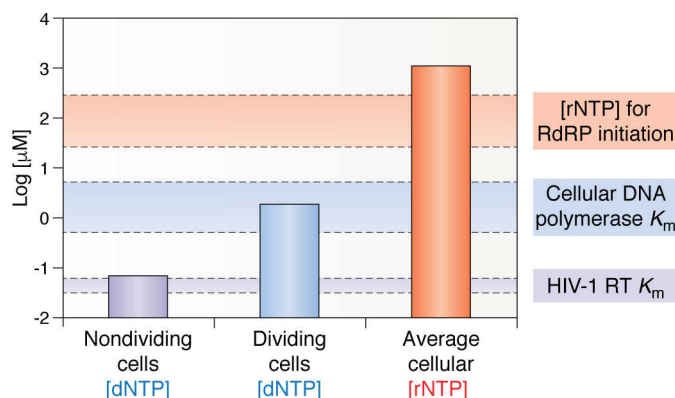


**Figure 1. Comparison of DNA and RNA polymerase steady-state kinetic activity and correlation with intracellular dNTP and rNTP concentrations.** The combined human replicative DNA polymerases ( $\alpha$ ,  $\delta$ , and  $\epsilon$ ) and HIV-1 RT  $K_m$  values (expressed as ranges consisting of reported mean  $K_m$  values, as described in Table 1) are denoted in reference to the plotted mean intracellular dNTPs found in dividing cells and nondividing cells (human monocyte-derived macrophages). rNTP concentrations found to be relatively high across cell types (20, 25) were plotted to be compared with the range of high rNTP concentrations required for initiation of viral RdRP polymerization described in text (Flaviviridae RdRP kinetics section) (107–109, 113, 114, 130, 131).

tive enzyme inhibitors. Utilizing the wealth of highly sensitive dNTP/rNTP measurement methods developed over time, creation of this resource, although requiring accurate measurement of cell volumes to yield units (cellular concentration) applicable to enzymology and pharmacology studies, would provide insight into the diverse and dynamic intracellular conditions present during animal studies and drug trials. As summarized in Fig. 1, cellular replicative DNA polymerases harbor  $K_m$  values close to the dNTP concentrations observed in dividing cells, making it possible that these  $K_m$  values might have been evolutionarily adapted for the optimal execution of DNA synthesis in dividing cells. However, lentiviral HIV-1 RT (Fig. 1) employs its uniquely low  $K_m$  values to complete proviral DNA synthesis and support viral replication in nondividing cells, such as macrophages, that are characterized by very poor dNTP availability. The highly abundant cellular rNTPs found across cell types enable RNA polymerases to efficiently initiate transcription and synthesize RNAs even with their demand for the high rNTP concentrations during the initiation of RNA synthesis (Fig. 1).

Whereas this review mainly focuses on the steady-state kinetic  $K_m$  values of polymerases, it is important to note that the catalytic rate ( $k_{\text{cat}}$ ) of polymerases can interplay with their  $K_m$  values to achieve overall optimal DNA and RNA synthesis in cells. In addition, when comparing intracellular dNTP/rNTP concentrations with polymerase kinetic parameters, it is important to note that variation in reported  $K_m$  values can arise through discrepancies in (i) template features (DNA versus RNA, sequence, length, and structure), (ii) reaction conditions (buffer components, pH, presence of all dNTPs versus one dNTP), (iii) polymerase origins (viral strains, purification methods), and (iv) modes of the polymerizations (initiation versus elongation). Similarly, when considering nucleotide/nucleoside inhibitor efficacy,  $\text{IC}_{50}$  data can vary, depending on viral polymerase subtypes and physiological  $\text{Mg}^{2+}$  concentrations (98, 146). In addition to the steady-state kinetic analyses, numerous

Nucleotides regulation status	Nucleotide concentrations	$K_m$ value ranges
[rNTP] Dividing/Nondividing cells Highly abundant Not cell cycle regulated	Very high (Near mM)	RNA polymerases (Initiation)
[dNTP] Dividing cells dNTP biosynthesis ↑ dNTP degradation ↓	High (Low μM)	Replicative DNA polymerases
[dNTP] Nondividing cells dNTP biosynthesis ↓ dNTP degradation ↑	Very low (Low nM)	Lentivirus reverse transcriptases

**Figure 2. Connections among nucleotide regulation status, cellular nucleotide levels, and enzyme kinetic values of polymerases.** Ranges of steady-state kinetic  $K_m$  values of DNA and RNA polymerases (orange) are arranged relative to cellular concentrations of their nucleotide substrates (blue). Intracellular nucleotide concentrations vary among cell types and are dependent upon differential metabolic regulations (green).

structural and mechanistic investigations (*i.e.* pre-steady-state kinetic studies) of polymerases elucidated highly orchestrated and dynamic molecular actions of enzymatic DNA and RNA synthesis. Overall, despite variations in data resulting from experimental disparities, cellular and viral polymerases appear to have been evolutionarily optimized to efficiently perform DNA and RNA synthesis within the cellular dNTP and rNTP concentrations naturally available during polymerization (Fig. 2). With this, it is plausible that the cellular dNTP concentrations, which significantly vary, depending on metabolic balance between dNTP biosynthesis and degradation (Fig. 2), may have driven the enzyme kinetic variations among DNA polymerases. Finally, this evolutionary cross-talk between polymerase enzyme kinetics and cellular nucleotide substrate availability is an important concept platform for the discovery of polymerase inhibitors.

**Funding and additional information**—This work was supported by National Institutes of Health Grant A1136581 (to B.K.), A1150451 (to B.K.), and MH116695 (to R.F.S.). The content is solely the responsibility of the authors and does not necessarily represent the official views of the National Institutes of Health.

**Conflict of interest**—The authors declare that they have no conflicts of interest with the contents of this article.

**Abbreviations**—The abbreviations used are: pol, polymerase; EBV, Epstein-Barr virus; HBV, hepatitis B virus; RT, reverse transcriptase; MuLV, murine leukemia virus; AMV, avian myeloblastosis virus; NRTI, nucleotide/nucleoside reverse transcriptase inhibitor; AZT-TP, 3'-azido-3'-deoxythymidine 5'-triphosphate; ddCTP, dideoxycytosine; ddITP, didanosine; TFV-DP, tenofovir; EFdA-TP, 4'-ethynyl-2-fluoro-2'-deoxyadenosine triphosphate; RdRP, RNA-dependent RNA polymerase; HCV, hepatitis C virus; IAV, influenza A virus; TP, triphosphate; DENV, dengue virus; MERS, Middle East respiratory syndrome; SARS, severe acute respiratory syndrome; CoV, coronavirus; 2'CM-ATP, 2'-C-methyl-ATP.

## References

- Kao, C. C., Singh, P., and Ecker, D. J. (2001) *De novo* initiation of viral RNA-dependent RNA synthesis. *Virology* **287**, 251–260 [CrossRef Medline](#)
- van Dijk, A. A., Makeyev, E. V., and Bamford, D. H. (2004) Initiation of viral RNA-dependent RNA polymerization. *J. Gen. Virol.* **85**, 1077–1093 [CrossRef Medline](#)
- Joyce, C. M., and Benkovic, S. J. (2004) DNA polymerase fidelity: kinetics, structure, and checkpoints. *Biochemistry* **43**, 14317–14324 [CrossRef Medline](#)
- Paul, A. V., van Boom, J. H., Filippov, D., and Wimmer, E. (1998) Protein-primed RNA synthesis by purified poliovirus RNA polymerase. *Nature* **393**, 280–284 [CrossRef Medline](#)
- Blumenthal, T. (1980) Q $\beta$  replicase template specificity: different templates require different GTP concentrations for initiation. *Proc. Natl. Acad. Sci. U. S. A.* **77**, 2601–2605 [CrossRef Medline](#)
- Lesburg, C. A., Cable, M. B., Ferrari, E., Hong, Z., Mannarino, A. F., and Weber, P. C. (1999) Crystal structure of the RNA-dependent RNA polymerase from hepatitis C virus reveals a fully encircled active site. *Nat. Struct. Biol.* **6**, 937–943 [CrossRef Medline](#)
- Li, Y., Mitaxov, V., and Waksman, G. (1999) Structure-based design of Taq DNA polymerases with improved properties of dideoxynucleotide incorporation. *Proc. Natl. Acad. Sci. U. S. A.* **96**, 9491–9496 [CrossRef Medline](#)
- Patra, A., Zhang, Q., Lei, L., Su, Y., Egli, M., and Guengerich, F. P. (2015) Structural and kinetic analysis of nucleoside triphosphate incorporation opposite an abasic site by human translesion DNA polymerase  $\eta$ . *J. Biol. Chem.* **290**, 8028–8038 [CrossRef Medline](#)
- O'Flaherty, D. K., and Guengerich, F. P. (2014) Steady-state kinetic analysis of DNA polymerase single-nucleotide incorporation products. *Curr. Protoc. Nucleic Acid Chem.* **59**, 7.21.1–7.21.13 [CrossRef Medline](#)
- Joyce, C. M. (2010) Techniques used to study the DNA polymerase reaction pathway. *Biochim. Biophys. Acta* **1804**, 1032–1040 [CrossRef Medline](#)
- Engstrom, Y., Eriksson, S., Jildevik, I., Skog, S., Thelander, L., and Tribukait, B. (1985) Cell cycle-dependent expression of mammalian ribonucleotide reductase: differential regulation of the two subunits. *J. Biol. Chem.* **260**, 9114–9116
- Coppock, D. L., and Pardee, A. B. (1987) Control of thymidine kinase mRNA during the cell cycle. *Mol. Cell Biol.* **7**, 2925–2932 [CrossRef Medline](#)
- Reichard, P. (1985) Ribonucleotide reductase and deoxyribonucleotide pools. *Basic Life Sci.* **31**, 33–45 [CrossRef Medline](#)
- Reichard, P. (1988) Interactions between deoxyribonucleotide and DNA synthesis. *Annu. Rev. Biochem.* **57**, 349–374 [CrossRef Medline](#)
- Franzolin, E., Pontarin, G., Rampazzo, C., Miazzi, C., Ferraro, P., Palumbo, E., Reichard, P., and Bianchi, V. (2013) The deoxynucleotide triphosphohydrolase SAMHD1 is a major regulator of DNA precursor pools in mammalian cells. *Proc. Natl. Acad. Sci. U. S. A.* **110**, 14272–14277 [CrossRef Medline](#)
- Schott, K., Fuchs, N. V., Derua, R., Mahboubi, B., Schnellbacher, E., Seifried, J., Tondera, C., Schmitz, H., Shepard, C., Brandariz-Nuñez, A., Diaz-Griffero, F., Reuter, A., Kim, B., Janssens, V., and König, R. (2018) Dephosphorylation of the HIV-1 restriction factor SAMHD1 is mediated by PP2A-B55 $\alpha$  holoenzymes during mitotic exit. *Nat. Commun.* **9**, 2227 [CrossRef Medline](#)
- Lee, E. J., Seo, J. H., Park, J. H., Vo, T. T. L., An, S., Bae, S. J., Le, H., Lee, H. S., Wee, H. J., Lee, D., Chung, Y. H., Kim, J. A., Jang, M. K., Ryu, S. H., Yu, E., *et al.* (2017) SAMHD1 acetylation enhances its deoxynucleotide triphosphohydrolase activity and promotes cancer cell proliferation. *Oncotarget* **8**, 68517–68529 [CrossRef Medline](#)
- Fairman, J. W., Wijerathna, S. R., Ahmad, M. F., Xu, H., Nakano, R., Jha, S., Prendergast, J., Welin, R. M., Flodin, S., Roos, A., Nordlund, P., Li, Z., Walz, T., and Dealwis, C. G. (2011) Structural basis for allosteric regulation of human ribonucleotide reductase by nucleotide-induced oligomerization. *Nat. Struct. Mol. Biol.* **18**, 316–322 [CrossRef Medline](#)



19. Zhu, C. F., Wei, W., Peng, X., Dong, Y. H., Gong, Y., and Yu, X. F. (2015) The mechanism of substrate-controlled allosteric regulation of SAMHD1 activated by GTP. *Acta Crystallogr. D Biol. Crystallogr.* **71**, 516–524 [CrossRef Medline](#)
20. Traut, T. W. (1994) Physiological concentrations of purines and pyrimidines. *Mol. Cell Biochem.* **140**, 1–22 [CrossRef Medline](#)
21. Diamond, T. L., Roshal, M., Jamburuthugoda, V. K., Reynolds, H. M., Merriam, A. R., Lee, K. Y., Balakrishnan, M., Bambara, R. A., Planelles, V., Dewhurst, S., and Kim, B. (2004) Macrophage tropism of HIV-1 depends on efficient cellular dNTP utilization by reverse transcriptase. *J. Biol. Chem.* **279**, 51545–51553 [CrossRef Medline](#)
22. Reardon, J. E. (1989) Herpes simplex virus type 1 and human DNA polymerase interactions with 2'-deoxyguanosine 5'-triphosphate analogues: kinetics of incorporation into DNA and induction of inhibition. *J. Biol. Chem.* **264**, 19039–19044 [Medline](#)
23. Copeland, W. C., Chen, M. S., and Wang, T. S. (1992) Human DNA polymerases  $\alpha$  and  $\beta$  are able to incorporate anti-HIV deoxynucleotides into DNA. *J. Biol. Chem.* **267**, 21459–21464 [Medline](#)
24. Starnes, M. C., and Cheng, Y. C. (1987) Cellular metabolism of 2',3'-dideoxycytidine, a compound active against human immunodeficiency virus *in vitro*. *J. Biol. Chem.* **262**, 988–991 [Medline](#)
25. Daikoku, T., Yamamoto, N., Saito, S., Kitagawa, M., Shimada, N., and Nishiyama, Y. (1991) Mechanism of inhibition of human cytomegalovirus replication by oxetanocin G. *Biochem. Biophys. Res. Commun.* **176**, 805–812 [CrossRef Medline](#)
26. Kamiya, H., and Kasai, H. (1995) Formation of 2-hydroxydeoxyadenosine triphosphate, an oxidatively damaged nucleotide, and its incorporation by DNA polymerases: steady-state kinetics of the incorporation. *J. Biol. Chem.* **270**, 19446–19450 [CrossRef Medline](#)
27. Fisher, P. A., Wang, T. S., and Korn, D. (1979) Enzymological characterization of DNA polymerase  $\alpha$ : basic catalytic properties processivity, and gap utilization of the homogeneous enzyme from human KB cells. *J. Biol. Chem.* **254**, 6128–6137 [Medline](#)
28. Dieckman, L. M., Johnson, R. E., Prakash, S., and Washington, M. T. (2010) Pre-steady state kinetic studies of the fidelity of nucleotide incorporation by yeast DNA polymerase delta. *Biochemistry* **49**, 7344–7350 [CrossRef Medline](#)
29. Einolf, H. J., and Guengerich, F. P. (2000) Kinetic analysis of nucleotide incorporation by mammalian DNA polymerase  $\delta$ . *J. Biol. Chem.* **275**, 16316–16322 [CrossRef Medline](#)
30. Cheng, C. H., and Kuchta, R. D. (1993) DNA polymerase epsilon: aphidicolin inhibition and the relationship between polymerase and exonuclease activity. *Biochemistry* **32**, 8568–8574 [CrossRef Medline](#)
31. Syvaaja, J., and Linn, S. (1989) Characterization of a large form of DNA polymerase  $\delta$  from HeLa cells that is insensitive to proliferating cell nuclear antigen. *J. Biol. Chem.* **264**, 2489–2497 [Medline](#)
32. Allaudeen, H. S., Kozarich, J. W., Bertino, J. R., and De Clercq, E. (1981) On the mechanism of selective inhibition of herpesvirus replication by (E)-5-(2-bromovinyl)-2'-deoxyuridine. *Proc. Natl. Acad. Sci. U. S. A.* **78**, 2698–2702 [CrossRef Medline](#)
33. Foster, S. A., Cerny, J., and Cheng, Y. C. (1991) Herpes simplex virus-specified DNA polymerase is the target for the antiviral action of 9-(2-phosphonylmethoxyethyl)adenine. *J. Biol. Chem.* **266**, 238–244 [Medline](#)
34. Mao, J. C., and Robishaw, E. E. (1975) Mode of inhibition of herpes simplex virus DNA polymerase by phosphonoacetate. *Biochemistry* **14**, 5475–5479 [CrossRef Medline](#)
35. Derse, D., Cheng, Y. C., Furman, P. A., St Clair, M. H., and Elion, G. B. (1981) Inhibition of purified human and herpes simplex virus-induced DNA polymerases by 9-(2-hydroxyethoxymethyl)guanine triphosphate: effects on primer-template function. *J. Biol. Chem.* **256**, 11447–11451 [Medline](#)
36. Allaudeen, H. S. (1985) Distinctive properties of DNA polymerases induced by herpes simplex virus type-1 and Epstein-Barr virus. *Antiviral Res.* **5**, 1–12 [CrossRef Medline](#)
37. Meisel, H., Reimer, K., von Janta-Lipinski, M., Bärwolf, D., and Matthes, E. (1990) Inhibition of hepatitis B virus DNA polymerase by 3'-fluorothymidine triphosphate and other modified nucleoside triphosphate analogs. *J. Med. Virol.* **30**, 137–141 [CrossRef Medline](#)
38. Park, S. G., Kim, Y., Park, E., Ryu, H. M., and Jung, G. (2003) Fidelity of hepatitis B virus polymerase. *Eur. J. Biochem.* **270**, 2929–2936 [CrossRef Medline](#)
39. Oh, S. H., Park, Y. H., and Woo, K. (1989) Inactivation of human hepatitis B virus DNA polymerase by pyridoxal 5'-phosphate. *J. Med. Virol.* **28**, 42–46 [CrossRef Medline](#)
40. Matthes, E., Reimer, K., von Janta-Lipinski, M., Meisel, H., and Lehmann, C. (1991) Comparative inhibition of hepatitis B virus DNA polymerase and cellular DNA polymerases by triphosphates of sugar-modified 5-methyldeoxycytidines and of other nucleoside analogs. *Antimicrob. Agents Chemother.* **35**, 1254–1257 [CrossRef Medline](#)
41. Kopp, E. B., Miglietta, J. J., Shrutkowski, A. G., Shih, C. K., Grob, P. M., and Skoog, M. T. (1991) Steady state kinetics and inhibition of HIV-1 reverse transcriptase by a non-nucleoside dipyrroldiazepinone, BI-RG-587, using a heteropolymeric template. *Nucleic Acids Res.* **19**, 3035–3039 [CrossRef Medline](#)
42. Woodside, A. M., and Guengerich, F. P. (2002) Effect of the O6 substituent on misincorporation kinetics catalyzed by DNA polymerases at O<sup>6</sup>-methylguanine and O<sup>6</sup>-benzylguanine. *Biochemistry* **41**, 1027–1038 [CrossRef Medline](#)
43. Furge, L. L., and Guengerich, F. P. (1997) Analysis of nucleotide insertion and extension at 8-oxo-7,8-dihydroguanine by replicative T7 polymerase exo- and human immunodeficiency virus-1 reverse transcriptase using steady-state and pre-steady-state kinetics. *Biochemistry* **36**, 6475–6487 [CrossRef Medline](#)
44. Gandhi, V. V., and Samuels, D. C. (2011) A review comparing deoxyribonucleoside triphosphate (dNTP) concentrations in the mitochondrial and cytoplasmic compartments of normal and transformed cells. *Nucleosides Nucleotides Nucleic Acids* **30**, 317–339 [CrossRef Medline](#)
45. Skoog, L., and Bjursell, G. (1974) Nuclear and cytoplasmic pools of deoxyribonucleoside triphosphates in Chinese hamster ovary cells. *J. Biol. Chem.* **249**, 6434–6438 [Medline](#)
46. Jackson, R. C., Lui, M. S., Boritzki, T. J., Morris, H. P., and Weber, G. (1980) Purine and pyrimidine nucleotide patterns of normal, differentiating, and regenerating liver and of hepatomas in rats. *Cancer Res.* **40**, 1286–1291 [Medline](#)
47. Mathews, C. K. (2015) Deoxyribonucleotide metabolism, mutagenesis and cancer. *Nat. Rev. Cancer* **15**, 528–539 [CrossRef Medline](#)
48. Schmidt, S., Schenkova, K., Adam, T., Erikson, E., Lehmann-Koch, J., Seritel, S., Verhasselt, B., Fackler, O. T., Lasitschka, F., and Keppler, O. T. (2015) SAMHD1's protein expression profile in humans. *J. Leukoc. Biol.* **98**, 5–14 [CrossRef Medline](#)
49. Jin, C., Peng, X., Liu, F., Cheng, L., Lu, X., Yao, H., Wu, H., and Wu, N. (2014) MicroRNA-181 expression regulates specific post-transcriptional level of SAMHD1 expression *in vitro*. *Biochem. Biophys. Res. Commun.* **452**, 760–767 [CrossRef Medline](#)
50. Bester, A. C., Roniger, M., Oren, Y. S., Im, M. M., Sarni, D., Chaoat, M., Bensimon, A., Zamir, G., Shewach, D. S., and Kerem, B. (2011) Nucleotide deficiency promotes genomic instability in early stages of cancer development. *Cell* **145**, 435–446 [CrossRef Medline](#)
51. Huang, C. Y., Yagüe-Capilla, M., González-Pacanoska, D., and Chang, Z. F. (2020) Quantitation of deoxynucleoside triphosphates by click reactions. *Sci. Rep.* **10**, 611 [CrossRef Medline](#)
52. Kuskovsky, R., Buj, R., Xu, P., Hofbauer, S., Doan, M. T., Jiang, H., Bostwick, A., Mesaros, C., Aird, K. M., and Snyder, N. W. (2019) Simultaneous isotope dilution quantification and metabolic tracing of deoxyribonucleotides by liquid chromatography high resolution mass spectrometry. *Anal. Biochem.* **568**, 65–72 [CrossRef Medline](#)
53. Zhang, W., Tan, S., Paintsil, E., Dutschman, G. E., Gullen, E. A., Chu, E., and Cheng, Y. C. (2011) Analysis of deoxyribonucleotide pools in human cancer cell lines using a liquid chromatography coupled with tandem mass spectrometry technique. *Biochem. Pharmacol.* **82**, 411–417 [CrossRef Medline](#)
54. Ferraro, P., Franzolin, E., Pontarin, G., Reichard, P., and Bianchi, V. (2010) Quantitation of cellular deoxynucleoside triphosphates. *Nucleic Acids Res.* **38**, e85 [CrossRef Medline](#)
55. Loeb, L. A., and Monnat, R. J., Jr. (2008) DNA polymerases and human disease. *Nat. Rev. Genet.* **9**, 594–604 [CrossRef Medline](#)

56. Gallo, R. C. (1972) Analytical review: RNA-dependent DNA polymerase in viruses and cells: views on the current state. *Blood* **39**, 117–137 [CrossRef](#)
57. Lujan, S. A., Williams, J. S., and Kunkel, T. A. (2016) DNA polymerases divide the labor of genome replication. *Trends Cell Biol.* **26**, 640–654 [CrossRef](#) [Medline](#)
58. Tan, C. K., Castillo, C., So, A. G., and Downey, K. M. (1986) An auxiliary protein for DNA polymerase- $\delta$  from fetal calf thymus. *J. Biol. Chem.* **261**, 12310–12316
59. Mondol, T., Stodola, J. L., Galletto, R., and Burgers, P. M. (2019) PCNA accelerates the nucleotide incorporation rate by DNA polymerase  $\delta$ . *Nucleic Acids Res.* **47**, 1977–1986 [CrossRef](#) [Medline](#)
60. Cherrington, J. M., Allen, S. J., McKee, B. H., and Chen, M. S. (1994) Kinetic analysis of the interaction between the diphosphate of (S)-1-(3-hydroxy-2-phosphonylmethoxypropyl)cytosine, ddCTP, AZTTP, and FlAUPT with human DNA polymerases  $\beta$  and  $\gamma$ . *Biochem. Pharmacol.* **48**, 1986–1988 [CrossRef](#) [Medline](#)
61. Vande Berg, B. J., Beard, W. A., and Wilson, S. H. (2001) DNA structure and aspartate 276 influence nucleotide binding to human DNA polymerase  $\beta$ : implication for the identity of the rate-limiting conformational change. *J. Biol. Chem.* **276**, 3408–3416 [CrossRef](#) [Medline](#)
62. Souza, T. M., De Souza, M. C., Ferreira, V. F., Canuto, C. V., Marques, I. P., Fontes, C. F., and Frugulhetti, I. C. (2008) Inhibition of HSV-1 replication and HSV DNA polymerase by the chloroquinolinic ribonucleoside 6-chloro-1,4-dihydro-4-oxo-1-( $\beta$ -D-ribofuranosyl) quino-line-3-carboxylic acid and its aglycone. *Antiviral Res.* **77**, 20–27 [CrossRef](#) [Medline](#)
63. Magee, W. C., Hostetler, K. Y., and Evans, D. H. (2005) Mechanism of inhibition of vaccinia virus DNA polymerase by cidofovir diphosphate. *Antimicrob. Agents Chemother.* **49**, 3153–3162 [CrossRef](#) [Medline](#)
64. McDonald, W. F., and Traktman, P. (1994) Overexpression and purification of the vaccinia virus DNA polymerase. *Protein Expr. Purif.* **5**, 409–421 [CrossRef](#) [Medline](#)
65. Xiong, X., Smith, J. L., Kim, C., Huang, E.-S., and Chen, M. S. (1996) Kinetic analysis of the interaction of cidofovir diphosphate with human cytomegalovirus DNA polymerase. *Biochem. Pharmacol.* **51**, 1563–1567 [CrossRef](#) [Medline](#)
66. Suzuki, S., Kimura, T., and Saneyoshi, M. (1986) Characterization of DNA polymerase induced by salmon herpesvirus, *Oncorhynchus masou* virus. *J. Gen. Virol.* **67**, 405–408 [CrossRef](#)
67. Suzuki, S., Misra, H. K., Wiebe, L. I., Knaus, E. E., and Tyrrell, D. L. (1987) A proposed mechanism for the selective inhibition of human cytomegalovirus replication by 1-(2'-deoxy-2'-fluoro- $\beta$ -D-arabinofuranosyl)-5-fluorouracil. *Mol. Pharmacol.* **31**, 301–306
68. Suzuki, S., Saneyoshi, M., Nakayama, C., Nishiyama, Y., and Yoshida, S. (1985) Mechanism of selective inhibition of human cytomegalovirus replication by 1- $\beta$ -D-arabinofuranosyl-5-fluorouracil. *Antimicrob. Agents Chemother.* **28**, 326–330 [CrossRef](#) [Medline](#)
69. Velpandi, A., Nagashunmugam, T., Murthy, S., Cartas, M., Monken, C., and Srinivasan, A. (1991) Generation of hybrid human immunodeficiency virus utilizing the cotransfection method and analysis of cellular tropism. *J. Virol.* **65**, 4847–4852 [CrossRef](#) [Medline](#)
70. Fenyo, E. M., Albert, J., and Asjo, B. (1989) Replicative capacity, cytopathic effect and cell tropism of HIV. *AIDS* **3**, S5–S12 [CrossRef](#) [Medline](#)
71. Connor, R. I., Sheridan, K. E., Ceradini, D., Choe, S., and Landau, N. R. (1997) Change in coreceptor use correlates with disease progression in HIV-1-infected individuals. *J. Exp. Med.* **185**, 621–628 [CrossRef](#) [Medline](#)
72. Risser, R., Horowitz, J. M., and McCubrey, J. (1983) Endogenous mouse leukemia viruses. *Annu. Rev. Genet.* **17**, 85–121 [CrossRef](#) [Medline](#)
73. Gallo, R. C., Poiesz, B. J., and Ruscetti, F. W. (1981) Regulation of human T-cell proliferation: T-cell growth factor and isolation of a new class of type-C retroviruses from human T-cells. *Haematol. Blood Transfus.* **26**, 502–514 [CrossRef](#) [Medline](#)
74. Weiss, R. A. (1987) Retroviruses and human disease. *J. Clin. Pathol.* **40**, 1064–1069 [CrossRef](#) [Medline](#)
75. Skasko, M., Weiss, K. K., Reynolds, H. M., Jamburuthugoda, V., Lee, K., and Kim, B. (2005) Mechanistic differences in RNA-dependent DNA polymerization and fidelity between murine leukemia virus and HIV-1 reverse transcriptases. *J. Biol. Chem.* **280**, 12190–12200 [CrossRef](#) [Medline](#)
76. Parker, W. B., White, E. L., Shaddix, S. C., Ross, L. J., Buckheit, R. W., Germany, J. M., Secrist, J. A., Vince, R., and Shannon, W. M. (1991) Mechanism of inhibition of human immunodeficiency virus type 1 reverse transcriptase and human DNA polymerases  $\alpha$ ,  $\beta$ , and  $\gamma$  by the 5'-triphosphates of carbovir, 3'-azido-3'-deoxythymidine, 2',3'-dideoxyguanosine and 3'-deoxythymidine: a novel RNA template for the evaluation of antiretroviral drugs. *J. Biol. Chem.* **266**, 1754–1762 [Medline](#)
77. Reardon, J. E., and Miller, W. H. (1990) Human immunodeficiency virus reverse transcriptase: substrate and inhibitor kinetics with thymidine 5'-triphosphate and 3'-azido-3'-deoxythymidine 5'-triphosphate. *J. Biol. Chem.* **265**, 20302–20307 [Medline](#)
78. Lenzi, G. M., Domaoal, R. A., Kim, D. H., Schinazi, R. F., and Kim, B. (2015) Mechanistic and kinetic differences between reverse transcriptases of Vpx coding and non-coding lentiviruses. *J. Biol. Chem.* **290**, 30078–30086 [CrossRef](#) [Medline](#)
79. Lenzi, G. M., Domaoal, R. A., Kim, D. H., Schinazi, R. F., and Kim, B. (2014) Kinetic variations between reverse transcriptases of viral protein X coding and noncoding lentiviruses. *Retrovirology* **11**, 111 [CrossRef](#) [Medline](#)
80. Coggins, S. A., Holler, J. M., Kimata, J. T., Kim, D. H., Schinazi, R. F., and Kim, B. (2019) Efficient pre-catalytic conformational change of reverse transcriptases from SAMHD1 non-counteracting primate lentiviruses during dNTP incorporation. *Virology* **537**, 36–44 [CrossRef](#) [Medline](#)
81. Kedar, P. S., Abbotts, J., Kovács, T., Lesiak, K., Torrence, P., and Wilson, S. H. (1990) Mechanism of HIV reverse transcriptase: enzyme-primer interaction as revealed through studies of a dNTP analogue, 3'-azido-dTTP. *Biochemistry* **29**, 3603–3611 [CrossRef](#) [Medline](#)
82. Wu, J. C., Chernow, M., Boehme, R. E., Suttman, R. T., McRoberts, M. J., Prisce, E. J., Matthews, T. R., Marx, P. A., Chuang, R. Y., and Chen, M. S. (1988) Kinetics and inhibition of reverse transcriptase from human and simian immunodeficiency viruses. *Antimicrob. Agents Chemother.* **32**, 1887–1890 [CrossRef](#) [Medline](#)
83. Furman, P. A., Fyfe, J. A., St Clair, M. H., Weinhold, K., Rideout, J. L., Freeman, G. A., Lehrman, S. N., Bolognesi, D. P., Broder, S., and Mitsuya, H. (1986) Phosphorylation of 3'-azido-3'-deoxythymidine and selective interaction of the 5'-triphosphate with human immunodeficiency virus reverse transcriptase. *Proc. Natl. Acad. Sci. U. S. A.* **83**, 8333–8337 [CrossRef](#) [Medline](#)
84. Huang, P., Farquhar, D., and Plunkett, W. (1990) Selective action of 3'-azido-3'-deoxythymidine 5'-triphosphate on viral reverse transcriptases and human DNA polymerases. *J. Biol. Chem.* **265**, 11914–11918 [Medline](#)
85. St Clair, M. H., Richards, C. A., Spector, T., Weinhold, K. J., Miller, W. H., Langlois, A. J., and Furman, P. A. (1987) 3'-Azido-3'-deoxythymidine triphosphate as an inhibitor and substrate of purified human immunodeficiency virus reverse transcriptase. *Antimicrob. Agents Chemother.* **31**, 1972–1977 [CrossRef](#) [Medline](#)
86. Nakane, H., and Ono, K. (1990) Differential inhibitory effects of some catechin derivatives on the activities of human immunodeficiency virus reverse transcriptase and cellular deoxyribonucleic and ribonucleic acid polymerases. *Biochemistry* **29**, 2841–2845 [CrossRef](#) [Medline](#)
87. Debyser, Z., Pauwels, R., Andries, K., Desmyter, J., Kukla, M., Janssen, P. A., and De Clercq, E. (1991) An antiviral target on reverse transcriptase of human immunodeficiency virus type 1 revealed by tetrahydroimidazo-[4,5,1-jk] [1,4]benzodiazepin-2 (1H)-one and -thione derivatives. *Proc. Natl. Acad. Sci. U. S. A.* **88**, 1451–1455 [CrossRef](#) [Medline](#)
88. Arion, D., Kaushik, N., McCormick, S., Borkow, G., and Parniak, M. A. (1998) Phenotypic mechanism of HIV-1 resistance to 3'-azido-3'-deoxythymidine (AZT): increased polymerization processivity and enhanced sensitivity to pyrophosphate of the mutant viral reverse transcriptase. *Biochemistry* **37**, 15908–15917 [CrossRef](#) [Medline](#)
89. Gu, Z., Fletcher, R. S., Arts, E. J., Wainberg, M. A., and Parniak, M. A. (1994) The K65R mutant reverse transcriptase of HIV-1 cross-resistant to 2', 3'-dideoxycytidine, 2',3'-dideoxy-3'-thiacytidine, and 2',3'-dideoxyinosine shows reduced sensitivity to specific dideoxynucleoside triphosphate inhibitors *in vitro*. *J. Biol. Chem.* **269**, 28118–28122 [Medline](#)

90. Quan, Y., Brenner, B. G., Marlink, R. G., Essex, M., Kurimura, T., and Wainberg, M. A. (2003) Drug resistance profiles of recombinant reverse transcriptases from human immunodeficiency virus type 1 subtypes A/E, B, and C. *AIDS Res. Hum. Retroviruses* **19**, 743–753 [CrossRef Medline](#)
91. Michailidis, E., Marchand, B., Kodama, E. N., Singh, K., Matsuoka, M., Kirby, K. A., Ryan, E. M., Sawani, A. M., Nagy, E., Ashida, N., Mitsuya, H., Parniak, M. A., and Sarafianos, S. G. (2009) Mechanism of inhibition of HIV-1 reverse transcriptase by 4'-ethynyl-2-fluoro-2'-deoxyadenosine triphosphate, a translocation-defective reverse transcriptase inhibitor. *J. Biol. Chem.* **284**, 35681–35691 [CrossRef Medline](#)
92. Hart, G. J., Orr, D. C., Penn, C. R., Figueiredo, H. T., Gray, N. M., Boehme, R. E., and Cameron, J. M. (1992) Effects of (–)-2'-deoxy-3'-thiacytidine (3TC) 5'-triphosphate on human immunodeficiency virus reverse transcriptase and mammalian DNA polymerases  $\alpha$ ,  $\beta$ , and  $\gamma$ . *Antimicrob. Agents Chemother.* **36**, 1688–1694 [CrossRef Medline](#)
93. Cihlar, T., Ray, A. S., Booramra, C. G., Zhang, L., Hui, H., Laflamme, G., Vela, J. E., Grant, D., Chen, J., Myrick, F., White, K. L., Gao, Y., Lin, K. Y., Douglas, J. L., Parkin, N. T., *et al.* (2008) Design and profiling of GS-9148, a novel nucleotide analog active against nucleoside-resistant variants of human immunodeficiency virus type 1, and its orally bioavailable phosphonoamidate prodrug, GS-9131. *Antimicrob. Agents Chemother.* **52**, 655–665 [CrossRef Medline](#)
94. Nakata, H., Amano, M., Koh, Y., Kodama, E., Yang, G., Bailey, C. M., Kohgo, S., Hayakawa, H., Matsuoka, M., Anderson, K. S., Cheng, Y. C., and Mitsuya, H. (2007) Activity against human immunodeficiency virus type 1, intracellular metabolism, and effects on human DNA polymerases of 4'-ethynyl-2-fluoro-2'-deoxyadenosine. *Antimicrob. Agents Chemother.* **51**, 2701–2708 [CrossRef Medline](#)
95. Hachiya, A., Kodama, E. N., Schuckmann, M. M., Kirby, K. A., Michailidis, E., Sakagami, Y., Oka, S., Singh, K., and Sarafianos, S. G. (2011) K70Q adds high-level tenofovir resistance to “Q151M complex” HIV reverse transcriptase through the enhanced discrimination mechanism. *PLoS ONE* **6**, e16242 [CrossRef Medline](#)
96. Tu, X., Das, K., Han, Q., Bauman, J. D., Clark, A. D., Jr., Hou, X., Frenkel, Y. V., Gaffney, B. L., Jones, R. A., Boyer, P. L., Hughes, S. H., Sarafianos, S. G., and Arnold, E. (2010) Structural basis of HIV-1 resistance to AZT by excision. *Nat. Struct. Mol. Biol.* **17**, 1202–1209 [CrossRef Medline](#)
97. Meyer, P. R., Matsuura, S. E., So, A. G., and Scott, W. A. (1998) Unblocking of chain-terminated primer by HIV-1 reverse transcriptase through a nucleotide-dependent mechanism. *Proc. Natl. Acad. Sci. U. S. A.* **95**, 13471–13476 [CrossRef Medline](#)
98. Njenda, D. T., Aralaguppe, S. G., Singh, K., Rao, R., Sönnnerborg, A., Sarafianos, S. G., and Neogi, U. (2018) Antiretroviral potency of 4'-ethynyl-2'-fluoro-2'-deoxyadenosine, tenofovir alafenamide and second-generation NNRTIs across diverse HIV-1 subtypes. *J. Antimicrob. Chemother.* **73**, 2721–2728 [CrossRef Medline](#)
99. Amie, S. M., Noble, E., and Kim, B. (2013) Intracellular nucleotide levels and the control of retroviral infections. *Virology* **436**, 247–254 [CrossRef Medline](#)
100. Aquaro, S., Perno, C. F., Balestra, E., Balzarini, J., Cenci, A., Francesconi, M., Panti, S., Serra, F., Villani, N., and Calì, R. (1997) Inhibition of replication of HIV in primary monocyte/macrophages by different antiviral drugs and comparative efficacy in lymphocytes. *J. Leukoc. Biol.* **62**, 138–143 [CrossRef Medline](#)
101. Nick McElhinny, S. A., Watts, B. E., Kumar, D., Watt, D. L., Lundström, E. B., Burgers, P. M., Johansson, E., Chabes, A., and Kunkel, T. A. (2010) Abundant ribonucleotide incorporation into DNA by yeast replicative polymerases. *Proc. Natl. Acad. Sci. U. S. A.* **107**, 4949–4954 [CrossRef Medline](#)
102. Buckstein, M. H., He, J., and Rubin, H. (2008) Characterization of nucleotide pools as a function of physiological state in *Escherichia coli*. *J. Bacteriol.* **190**, 718–726 [CrossRef Medline](#)
103. Zhong, W., Uss, A. S., Ferrari, E., Lau, J. Y., and Hong, Z. (2000) *De novo* initiation of RNA synthesis by hepatitis C virus nonstructural protein 5B polymerase. *J. Virol.* **74**, 2017–2022 [CrossRef Medline](#)
104. Nomaguchi, M., Ackermann, M., Yon, C., You, S., Padmanabhan, R., and Padmanabhan, R. (2003) *De novo* synthesis of negative-strand RNA by Dengue virus RNA-dependent RNA polymerase *in vitro*: nucleotide, primer, and template parameters. *J. Virol.* **77**, 8831–8842 [CrossRef Medline](#)
105. Tchesnokov, E. P., Raesisimakiani, P., Ngure, M., Marchant, D., and Götte, M. (2018) Recombinant RNA-dependent RNA polymerase complex of Ebola virus. *Sci. Rep.* **8**, 3970 [CrossRef Medline](#)
106. Gordon, C. J., Tchesnokov, E. P., Woolner, E., Perry, J. K., Feng, J. Y., Porter, D. P., and Götte, M. (2020) Remdesivir is a direct-acting antiviral that inhibits RNA-dependent RNA polymerase from severe acute respiratory syndrome coronavirus 2 with high potency. *J. Biol. Chem.* **295**, 6785–6797 [CrossRef Medline](#)
107. Stridh, S. (1983) Determination of ribonucleoside triphosphate pools in influenza A virus-infected MDCK cells. *Arch. Virol.* **77**, 223–229 [CrossRef Medline](#)
108. Haugen, S. P., Ross, W., and Gourse, R. L. (2008) Advances in bacterial promoter recognition and its control by factors that do not bind DNA. *Nat. Rev. Microbiol.* **6**, 507–519 [CrossRef Medline](#)
109. Browning, D. F., and Busby, S. J. (2004) The regulation of bacterial transcription initiation. *Nat. Rev. Microbiol.* **2**, 57–65 [CrossRef Medline](#)
110. Saecker, R. M., Record, M. T., Jr., and Dehaseth, P. L. (2011) Mechanism of bacterial transcription initiation: RNA polymerase–promoter binding, isomerization to initiation-competent open complexes, and initiation of RNA synthesis. *J. Mol. Biol.* **412**, 754–771 [CrossRef Medline](#)
111. Osumi-Davis, P. A., Sreerama, N., Volkin, D. B., Middaugh, C. R., Woody, R. W., and Woody, A. Y. (1994) Bacteriophage T7 RNA polymerase and its active-site mutants: kinetic, spectroscopic and calorimetric characterization. *J. Mol. Biol.* **237**, 5–19 [CrossRef Medline](#)
112. Bochner, B. R., and Ames, B. N. (1982) Complete analysis of cellular nucleotides by two-dimensional thin layer chromatography. *J. Biol. Chem.* **257**, 9759–9769 [CrossRef Medline](#)
113. Gardner, L. P., Mookhtiar, K. A., and Coleman, J. E. (1997) Initiation, elongation, and processivity of carboxyl-terminal mutants of T7 RNA polymerase. *Biochemistry* **36**, 2908–2918 [CrossRef Medline](#)
114. Ranjith-Kumar, C. T., Gutshall, L., Kim, M. J., Sarisky, R. T., and Kao, C. C. (2002) Requirements for *de novo* initiation of RNA synthesis by recombinant flaviviral RNA-dependent RNA polymerases. *J. Virol.* **76**, 12526–12536 [CrossRef Medline](#)
115. Ackermann, M., and Padmanabhan, R. (2001) *De novo* synthesis of RNA by the dengue virus RNA-dependent RNA polymerase exhibits temperature dependence at the initiation but not elongation phase. *J. Biol. Chem.* **276**, 39926–39937 [CrossRef Medline](#)
116. Jácome, R., Becerra, A., Ponce de León, S., and Lazcano, A. (2015) Structural analysis of monomeric RNA-dependent polymerases: evolutionary and therapeutic implications. *PLoS ONE* **10**, e0139001 [CrossRef Medline](#)
117. Ferrari, E., Wright-Minogue, J., Fang, J. W., Baroudy, B. M., Lau, J. Y., and Hong, Z. (1999) Characterization of soluble hepatitis C virus RNA-dependent RNA polymerase expressed in *Escherichia coli*. *J. Virol.* **73**, 1649–1654 [CrossRef Medline](#)
118. Bartschlagler, R., Ahlborn-Laake, L., Yasargil, K., Mous, J., and Jacobsen, H. (1995) Substrate determinants for cleavage in *cis* and in *trans* by the hepatitis C virus NS3 proteinase. *J. Virol.* **69**, 198–205 [CrossRef Medline](#)
119. Luo, G., Hamatake, R. K., Mathis, D. M., Racela, J., Rigat, K. L., Lemm, J., and Colonno, R. J. (2000) *De novo* initiation of RNA synthesis by the RNA-dependent RNA polymerase (NS5B) of hepatitis C virus. *J. Virol.* **74**, 851–863 [CrossRef Medline](#)
120. Kao, C. C., Del Vecchio, A. M., and Zhong, W. (1999) *De novo* initiation of RNA synthesis by a recombinant flaviviridae RNA-dependent RNA polymerase. *Virology* **253**, 1–7 [CrossRef Medline](#)
121. Ranjith-Kumar, C. T., Sarisky, R. T., Gutshall, L., Thomson, M., and Kao, C. C. (2004) *De novo* initiation pocket mutations have multiple effects on hepatitis C virus RNA-dependent RNA polymerase activities. *J. Virol.* **78**, 12207–12217 [CrossRef Medline](#)
122. Filomatori, C. V., Lodeiro, M. F., Alvarez, D. E., Samsa, M. M., Pietrasanta, L., and Gamarnik, A. V. (2006) A 5' RNA element promotes dengue virus RNA synthesis on a circular genome. *Genes Dev.* **20**, 2238–2249 [CrossRef Medline](#)
123. Selisko, B., Potisopon, S., Agred, R., Priet, S., Varlet, I., Thillier, Y., Sallamand, C., Debart, F., Vasseur, J. J., and Canard, B. (2012) Molecular basis

- for nucleotide conservation at the ends of the dengue virus genome. *PLoS Pathog.* **8**, e1002912 [CrossRef Medline](#)
124. Butcher, S. J., Grimes, J. M., Makeyev, E. V., Bamford, D. H., and Stuart, D. I. (2001) A mechanism for initiating RNA-dependent RNA polymerization. *Nature* **410**, 235–240 [CrossRef Medline](#)
  125. Egloff, M. P., Decroly, E., Malet, H., Selisko, B., Benarroch, D., Ferron, F., and Canard, B. (2007) Structural and functional analysis of methylation and 5'-RNA sequence requirements of short capped RNAs by the methyltransferase domain of dengue virus NS5. *J. Mol. Biol.* **372**, 723–736 [CrossRef Medline](#)
  126. Bressanelli, S., Tomei, L., Rey, F. A., and De Francesco, R. (2002) Structural analysis of the hepatitis C virus RNA polymerase in complex with ribonucleotides. *J. Virol.* **76**, 3482–3492 [CrossRef Medline](#)
  127. Yap, T. L., Xu, T., Chen, Y. L., Malet, H., Egloff, M. P., Canard, B., Vasudevan, S. G., and Lescar, J. (2007) Crystal structure of the dengue virus RNA-dependent RNA polymerase catalytic domain at 1.85-angstrom resolution. *J. Virol.* **81**, 4753–4765 [CrossRef Medline](#)
  128. Lohmann, V. (2013) Hepatitis C virus RNA replication. *Curr. Top. Microbiol. Immunol.* **369**, 167–198 [CrossRef Medline](#)
  129. Mosley, R. T., Edwards, T. E., Murakami, E., Lam, A. M., Grice, R. L., Du, J., Sofia, M. J., Furman, P. A., and Otto, M. J. (2012) Structure of hepatitis C virus polymerase in complex with primer-template RNA. *J. Virol.* **86**, 6503–6511 [CrossRef Medline](#)
  130. Harrus, D., Ahmed-El-Sayed, N., Simister, P. C., Miller, S., Triconnet, M., Hagedorn, C. H., Mahias, K., Rey, F. A., Astier-Gin, T., and Bressanelli, S. (2010) Further insights into the roles of GTP and the C terminus of the hepatitis C virus polymerase in the initiation of RNA synthesis. *J. Biol. Chem.* **285**, 32906–32918 [CrossRef Medline](#)
  131. Lim, S. P., Noble, C. G., Seh, C. C., Soh, T. S., El Sahili, A., Chan, G. K., Lescar, J., Arora, R., Benson, T., Nilar, S., Manjunatha, U., Wan, K. F., Dong, H., Xie, X., Shi, P. Y., *et al.* (2016) Potent allosteric Dengue virus NS5 polymerase inhibitors: mechanism of action and resistance profiling. *PLoS Pathog.* **12**, e1005737 [CrossRef Medline](#)
  132. Sesmero, E., and Thorpe, I. F. (2015) Using the hepatitis C virus RNA-dependent RNA polymerase as a model to understand viral polymerase structure, function and dynamics. *Viruses* **7**, 3974–3994 [CrossRef Medline](#)
  133. Bressanelli, S., Tomei, L., Roussel, A., Incitti, I., Vitale, R. L., Mathieu, M., De Francesco, R., and Rey, F. A. (1999) Crystal structure of the RNA-dependent RNA polymerase of hepatitis C virus. *Proc. Natl. Acad. Sci. U. S. A.* **96**, 13034–13039 [CrossRef Medline](#)
  134. Gao, G., Orlova, M., Georgiadis, M. M., Hendrickson, W. A., and Goff, S. P. (1997) Conferring RNA polymerase activity to a DNA polymerase: a single residue in reverse transcriptase controls substrate selection. *Proc. Natl. Acad. Sci. U. S. A.* **94**, 407–411 [CrossRef Medline](#)
  135. Selisko, B., Papageorgiou, N., Ferron, F., and Canard, B. (2018) Structural and functional basis of the fidelity of nucleotide selection by flavivirus RNA-dependent RNA polymerases. *Viruses* **10**, 59 [CrossRef Medline](#)
  136. Campagnola, G., McDonald, S., Beaucourt, S., Vignuzzi, M., and Peersen, O. B. (2015) Structure-function relationships underlying the replication fidelity of viral RNA-dependent RNA polymerases. *J. Virol.* **89**, 275–286 [CrossRef Medline](#)
  137. Vreede, F. T., Jung, T. E., and Brownlee, G. G. (2004) Model suggesting that replication of influenza virus is regulated by stabilization of replicative intermediates. *J. Virol.* **78**, 9568–9572 [CrossRef Medline](#)
  138. Kao, C. C., and Sun, J. H. (1996) Initiation of minus-strand RNA synthesis by the brome mosaicvirus RNA-dependent RNA polymerase: use of oligoribonucleotide primers. *J. Virol.* **70**, 6826–6830 [CrossRef Medline](#)
  139. Testa, D., and Banerjee, A. K. (1979) Initiation of RNA synthesis *in vitro* by vesicular stomatitis virus: role of ATP. *J. Biol. Chem.* **254**, 2053–2058 [Medline](#)
  140. Vreede, F. T., Gifford, H., and Brownlee, G. G. (2008) Role of initiating nucleoside triphosphate concentrations in the regulation of influenza virus replication and transcription. *J. Virol.* **82**, 6902–6910 [CrossRef Medline](#)
  141. Zhang, S., Weng, L., Geng, L., Wang, J., Zhou, J., Deubel, V., Buchy, P., and Toyoda, T. (2010) Biochemical and kinetic analysis of the influenza virus RNA polymerase purified from insect cells. *Biochem. Biophys. Res. Commun.* **391**, 570–574 [CrossRef Medline](#)
  142. Tchesnokov, E. P., Feng, J. Y., Porter, D. P., and Götte, M. (2019) Mechanism of inhibition of Ebola virus RNA-dependent RNA polymerase by remdesivir. *Viruses* **11**, 326 [CrossRef Medline](#)
  143. Gordon, C. J., Tchesnokov, E. P., Feng, J. Y., Porter, D. P., and Götte, M. (2020) The antiviral compound remdesivir potently inhibits RNA-dependent RNA polymerase from Middle East respiratory syndrome coronavirus. *J. Biol. Chem.* **295**, 4773–4779 [CrossRef Medline](#)
  144. Agostini, M. L., Andres, E. L., Sims, A. C., Graham, R. L., Sheahan, T. P., Lu, X., Smith, E. C., Case, J. B., Feng, J. Y., Jordan, R., Ray, A. S., Cihlar, T., Siegel, D., Mackman, R. L., Clarke, M. O., *et al.* (2018) Coronavirus susceptibility to the antiviral remdesivir (GS-5734) is mediated by the viral polymerase and the proofreading exoribonuclease. *mBio* **9**, e00221-18 [CrossRef Medline](#)
  145. Mumtaz, N., Jimmerson, L. C., Bushman, L. R., Kiser, J. J., Aron, G., Reusken, C., Koopmans, M. P. G., and van Kampen, J. J. A. (2017) Cell-line dependent antiviral activity of sofosbuvir against Zika virus. *Antiviral Res.* **146**, 161–163 [CrossRef Medline](#)
  146. Achuthan, V., Singh, K., and DeStefano, J. J. (2017) Physiological Mg<sup>2+</sup> conditions significantly alter the inhibition of HIV-1 and HIV-2 reverse transcriptases by nucleoside and non-nucleoside inhibitors *in vitro*. *Biochemistry* **56**, 33–46 [CrossRef Medline](#)